



Published in final edited form as:

Neurotoxicol Teratol. 2021 ; 88: 107037. doi:10.1016/j.ntt.2021.107037.

Latent effects of early-life methylmercury exposure on motor function in *Drosophila*

Ashley E. Peppriell, Jakob T. Gunderson, Ian N. Krout, Daria Vorojeikina, Matthew D. Rand
Department of Environmental Medicine, University of Rochester School of Medicine and Dentistry, Rochester, NY, USA

Abstract

The developmental toxicant, methylmercury (MeHg), can elicit motor deficits that last well into adulthood. Recent studies using *Drosophila* showed that the developing musculature is sensitive to high doses of MeHg, where a larval feeding paradigm resulted in compromised myotendinous junction (MTJ) formation during development, by a mechanism involving the NG2 homologue, *kon-tiki* (*kon*). Low-dose exposures to MeHg that do not produce muscle pathology during development, nevertheless result in impaired flight behavior later in adult life. The present study evaluated the potential for relatively low-dose exposure to produce latent adult muscle pathology and motor impairments, as assayed by climbing and flight, as well as to evaluate molecular mechanisms that may contribute to motor deficits. Wildtype larvae were fed 0 – 5 μ M MeHg laden food until eclosion. The effect of 5 μ M MeHg on MTJ-related gene expression during pupal development was assessed via quantitative RT-qPCR analysis. Upon eclosion, adults were transferred to standard food bottles for 4, 11, or 30 days prior to motor testing. Survivorship (%) was determined from a subset of 200 flies per treatment. Average climbing speed (cm/s) was quantified 4-days post-eclosion (PE). Flight ability was assayed 11- or 30-days PE by measuring landing height (cm) of flies dropped into an adhesive-lined vertical column. In parallel, total body mercury was measured to estimate the influence of residual MeHg at the time of motor testing. Muscle morphology was assessed using immuno-fluorescence microscopy. Exposure to 5 μ M MeHg significantly reduced climbing speed, and flight ability 4 and 11 – days PE, respectively. While age-related flight deficits were seen in each sex, flight deficits due to MeHg persisted to 30-day PE timepoints exclusively in males. Expression of *kon* was upregulated across the window of pupal development essential to establishing adult MTJ. However, experimentally restricting the induction of comparable levels of *kon* to muscle during the same periods did not recapitulate the flight deficits, indicating that muscle-specific induction of *kon* alone is not sufficient to contribute to latent flight impairments. Adult flight muscle morphology of 11-day PE flies treated with 5 μ M MeHg was indistinct from controls, implying muscle structure is not grossly perturbed to impair flight. Collectively, the current data suggest that developmental exposure to 5 μ M MeHg reduces flight ability in each sex at 11 day-PE and that latent deficits at 30-day PE are male-specific. It remains to be determined whether the developing MTJ of *Drosophila* is a sensitive target of

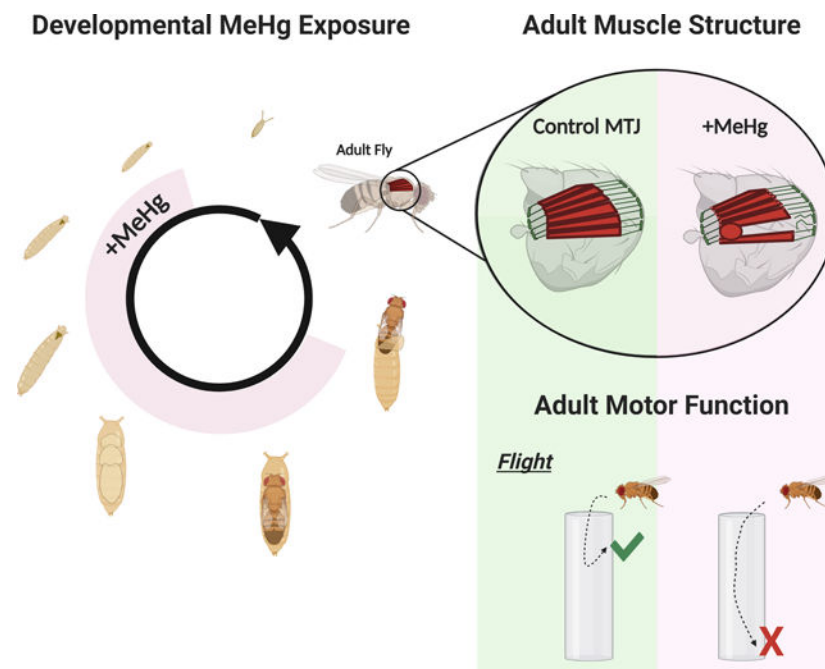
Corresponding Author: Ashley Peppriell, Ashley_peppriell@urmc.rochester.edu.

Conflict of Interest:

The authors have no conflicts of interest to declare.

MeHg, and whether or not *kon* acts in conjunction with additional MTJ factors to constitute a MeHg target.

Graphical Abstract:



To model gestational development of methylmercury (MeHg) *Drosophila* are exposed through food during a portion of their life-cycle shaded in pink until eclosion from the pupa case. Adult muscle structure and function are evaluated to discern latent toxicity of low-level exposures.

Keywords

Methylmercury; organometals; *Drosophila*; alternative models; behavioral outcomes; developmental toxicity

1. Introduction:

Methylmercury (MeHg) is a developmental toxicant of global public health concern (UN, 2019). Humans are predominantly exposed to MeHg in seafood, and communities that rely on fish as a main source of nutrients are disproportionately exposed (Malm et al., 1995; Marques et al., 2016; Sheehan et al., 2014). The developing fetus is especially sensitive to MeHg, as was exemplified after historical poisoning events in Japan and Iraq in the mid-20th century (Harada, 1995) (Bakir et al., 1973). More recent epidemiological studies of seafood-eating populations have focused on associations of prenatal mercury exposure with adverse cognitive and motor endpoints in children (Debes et al., 2006; Grandjean et al., 1997; Myers and Davidson, 1998; Sorensen et al., 1999). Inconsistent results across these cohorts suggest the need for the expansion of developmental assessments to additional outcomes in order to broaden our understanding of the developmental impacts of MeHg

toxicity; such efforts would ultimately improve the estimates of the risks arising from MeHg exposures.

An area of special concern is persistent and delayed toxicity, which the Environmental Protection Agency (EPA) recently identified as a key area in need of additional research (EPA., 2019). Follow-up studies of historical poisoning cases have demonstrated that developmental toxicity of MeHg can exhibit latent effects, also referred to as “silent toxicity” (Kinjo, 1993; Reuhl, 1991; Weiss et al., 2002; Yorifuji et al., 2018). The concept of latency is also reflected in principles of developmental origins of health and disease (DOHaD), where early-life exposures manifest as health effects later in life (Godfrey and Barker, 2001; Hanson and Gluckman, 2014).

Experimental animal studies have described cognitive and motor behavior deficits following MeHg exposure that manifest with age (Day et al., 2005; Newland et al., 2008; Newland and Rasmussen, 2000; Newland et al., 2004; Rice, 1996). One study of monkeys exposed to MeHg during post-natal development described a delayed neurotoxicity that was exhibited 13 years later as, “clumsiness and slowness in reaching for objects” (Rice, 1996). Adult-onset behavioral neurotoxicity following developmental MeHg exposure has also been described in the rodent literature (Montgomery et al., 2008; Newland et al., 2015) (Day et al., 2005; Newland and Rasmussen, 2000; Spyker et al., 1972) as well as in alternative model organisms such as *C.elegans* (Ke et al., 2021). Many of the aforementioned studies ascribe an exclusively neurotoxic mechanism to the latent neuromuscular sequelae of MeHg. However, it is now known that other organ systems are sensitive to MeHg, including the immune, cardiovascular, and musculoskeletal systems (Hong et al., 2012; Karagas et al., 2012). To understand the latent effects of MeHg toxicity more completely, and fill existing knowledge gaps, it is crucial to consider the contributions and involvement of other organ systems and tissues in the adverse consequences of MeHg exposure.

Indeed, MeHg can directly impact the musculoskeletal system, which may contribute to motor deficits. Smaller fiber diameter and reduced mitochondrial enzyme activity were observed in a histopathological study of skeletal muscle in rats exposed to high levels (5 mg/kg/day) of MeHg (Usuki et al., 1998). A similar study using Zebrafish observed reduced muscle fiber size as well (de Oliveira Ribeiro et al., 2008). Reduction in fiber diameter would theoretically reduce the surface area of contact between muscle and tendon, weakening the MTJ by reducing its capacity to transmit force, thereby making it more susceptible to injury (Jakobsen and Krogsgaard, 2021; Trotter et al., 1985). A recent rodent study using a developmental exposure paradigm and lower doses (0 – 5.0 ppm MeHg in drinking water) observed adult motor deficits that paralleled a preferential accumulation of T-Hg in muscle tissue. The motor impairments were not accompanied by an overt histopathology at the level of the skeletal muscle fibers (Rand et al., 2020). However, the study did not assess the possibility that pathology extends to other muscle structures or manifests later in life, after muscles endure additional functional strain with age.

Studies in *Drosophila* have modelled gestational exposure to MeHg and shown that toxicity is elicited somewhat selectively in developing muscle. Recent studies from our laboratory have unveiled muscle-specific mechanisms that are susceptible to developmental MeHg

exposure and contribute to motor behavioral deficits (Gunderson et al., 2020; Peppriell et al., 2020; Prince and Rand, 2017). In one recent investigation, high doses of MeHg compromised the formation of the indirect flight muscle (IFM) in a manner consistent with a failure in myotendinous junction (MTJ) formation (Peppriell et al., 2020). In contrast to the overt muscle detachment phenotypes observed with high doses in the food (10 μ M and above), relatively lower doses (5 μ M and below) did not lead to muscle pathology in developing flies. Nevertheless, the flies at the lower dose exhibited stark decrements in adult flight ability later in life (Peppriell et al., 2020). Yet, the potential for latent effects in adults following low-dose MeHg exposure during development remains to be characterized.

Here, we sought to leverage the *Drosophila* model to investigate the paradigm of early-life exposure to MeHg for latent effects on the adult muscle and motor behaviors and to provide a platform to elucidate the underlying molecular targets.

2. Methods:

2.1 *Drosophila* strains and methods:

The following fly strains were obtained from the Bloomington *Drosophila* Stock Center at Indiana University (Bloomington, Indiana): *Canton S* (#1) and *w¹¹¹⁸* (#5905). The UAS-HA-kon-FL4-1/TM3 (“kon-HA”), *wg-lacZ* was a gift of F. Schnorrer (Max Planck Institute of Biochemistry, Martinsried, Germany). These flies contain the full length kon coding sequence with the addition of the wingless (*wg*) signal peptide (F.S. personal communication). Overexpression and knockdown studies were performed using the Gal4/UAS system (Brand and Perrimon, 1993). The Mef2-GAL4 line carrying a GAL80 gene (Mef2-GAL4-GAL80-ts) for temperature regulated expression was gifted from the Bohmann lab (University of Rochester). All crosses were performed between respective virgin female GAL4 lines and male UAS lines or the control line (*w¹¹¹⁸*). All stock lines were maintained on a standard fly food made of cornmeal, molasses, yeast, and agar, prepared in a centralized facility in the Department of Molecular Genetics, University of Rochester. All experimental treatments with MeHg were prepared using Jazz Mix *Drosophila* food (Fisher Scientific, #AS153) prepared freshly in the Rand lab. Flies were maintained in a humidified chamber at 25°C on a 12/12hr light/dark cycle.

2.2 Methylmercury exposure paradigms

2.2.1 Developmental exposure – motor testing—First-instar (L1) *Canton S*. (CS) larvae were seeded at 300/bottle into food containing 0, 2.5, or 5 μ M MeHg (methylmercury chloride, Sigma-Aldrich # 215465), and allowed to develop to specific stages of pupariation (described below) for RNA collection or continue until eclosion of adults. Upon eclosion, adult flies were separated by sex and moved to MeHg-free food until motor function testing at 4-, 11-, or 30-days post eclosion (PE), or dissection at 11-day PE in preparation for immunohistochemistry analysis described below. A third subset of adult flies was collected at 4-, 11-, or 30-days PE to determine total body mercury levels (T-Hg) described below. The exposure paradigm is shown in Figure 1A.

2.2.2 Adult exposure – motor testing—Freshly-eclosed CS adult flies were separated by sex and moved to food containing 0, 10, or 50 μM MeHg until motor function testing at 4-, or 11-days PE. A second subset of adult flies was collected at corresponding timepoints to determine total body mercury levels (T-Hg) described below. The exposure paradigm is shown in Figure 1B.

2.3 Longevity Tests

Longevity, the measure of adult lifespan, was assayed under two exposure paradigms: during development (larval to pupal stages) and during the adult stage. Longevity assays were restricted to male flies, due to the variability that female flies typically exhibit in this assay (Iliadi et al., 2009). For the developmental exposure, CS L1 larvae were introduced to food with various concentrations of MeHg (0 – 5 μM) and allowed to grow through metamorphosis. Upon eclosion, 200 male flies from each treatment group were collected and transferred to MeHg-free food vials and separated in four replicate vials (50 males/vial). Flies were transferred to fresh food vials every 2–3 days, at which point the number of dead flies were scored. Cultures were maintained until all the flies had died.

For the adult-specific exposure, CS larvae were reared on MeHg-free food and adults collected within a day post eclosion. Adults were introduced to food with various concentrations of MeHg (0 – 100 μM) in four replicate vials (50 males/vial) and maintained on those concentrations throughout their lifespan. Untreated (0 μM) CS flies served as controls in all cases. Flies were transferred to fresh food vials containing the respective MeHg concentration every 2–3 days, at which point the number of dead flies were scored. Cultures were maintained until all the flies had died.

Data are displayed as Survivorship (%). Results from four technical replicates were pooled to generate average survivorship curves. Mean lifespan and statistical analysis of longevity difference was performed using Online Application for Survival Analysis OASIS 2 (Oasis 2 website <https://sbi.postech.ac.kr/oasis2/history/>)(Han et al., 2016). Kaplan-Meier survival curves were constructed to display lifespan data and Mantel-Cox log-rank statistical analysis was used for testing significance between survivorship curves.

2.4 Adult motor function analyses

2.4.1 Climbing speed (cm/s) assessment: Climbing (negative geotaxis) experiments were performed with minor modifications from those previously described (Gargano et al., 2005), with climbing behavior recorded on video. Briefly, adult flies were collected upon eclosion and aged for four days. To test for climbing, batches of 10 flies were transferred into a clear, empty, 2.5 cm diameter polystyrene vial demarcated with 1 cm increments from the bottom. The vial was gently tapped so that the flies fell to the bottom. Video recordings lasting 15 s each captured the duration of time for each fly to traverse a four cm vertical distance, which was logged as speed (cm/s). Three videos were recorded for each sex and treatment group. Average \pm standard deviation was determined from 10 flies per video. Flies that did not perform the behavior were censored (not scored).

2.4.2 Flight assessment—Flight tests were performed with minor modifications to those previously described (Babcock and Ganetzky, 2014). The dimensions of the plexi-glass flight column (76.2 cm, 12.7cm diameter, 34 cm circumference and drop column 25.5 cm, 3.2 cm diameter, 10.2 cm circumference) were maintained from Babcock and Ganetzky's apparatus, while the funnel and tubes were adjusted for our setup. The diameter of the funnel was 2.3 cm which was flush with the plastic food vials (2.5 cm) used to transmit the flies down the drop column one vial at a time through the funnel and ultimately into the flight column. The flight column was lined with a removable acrylic sheet with paintable adhesive (TangleFoot, Tangle-Trap Inc.) to capture flies where they alight after entering the column. The landing height of a fly corresponds to the fitness in flight performance. The adhesive liner was removed to a white surface, imaged, and the landing heights of at least 50 flies per group were digitally quantified. Landing heights of individual flies are represented in cm. Flies which fell to the bottom, captured in a mineral oil dish, were categorized as "flightless" and were recorded but censored (not scored) from landing height analysis. Before testing, freshly eclosed adult males and females were separated on CO₂ and recovered for at least 24 h. Flies were tested 11 days PE or 30-day PE where indicated. Flies were kept at 25°C throughout the exposure and recovery periods leading up to testing. All flies were tested between 10AM and 12PM to control for physiological influences of the circadian behaviors.

2.5 Evaluation of adult muscle morphology

Following developmental exposure to 0 or 5 µM MeHg, 11-day PE female *CS* adult thoraces were prepared for histology and immunohistochemical (IHC) staining as described by Weitkunat and Schnorrer with minor modifications (Weitkunat and Schnorrer, 2014). Briefly, thoraces were dissected from head and abdomen using a razor blade. Thoraces were then fixed in Methacarn fixative (Methanol/Chloroform/Acetic acid in a 6:3:1 ratio) for 1 h at room temperature. Thoraces were sequentially rehydrated in a methanol:PBS series (80:20, 70:30, 50:50, 30:70, 100% PBS, 10 minutes each) and finally into PBS, 0.1% tween-20 (PBST) buffer, and then bisected using a scalpel blade (Feather, #504169) along the dorsal midline to expose the six dorsal longitudinal muscle (DLM) fibers on each hemithorax before being placed into a 24-well plate with PBS. Hemithoraces were washed once with PBS, blocked 1:1 AquaBlock (EastCoast Bio, #PP82): PBS for 1 h, then incubated overnight at 4 °C with mouse anti-BPS-integrin primary antibody (Developmental Studies Hybridoma Bank, # CF6G.11, antibody concentration was 1 µg/ml). The next day, the hemithoraces were washed and incubated for 2 h at 4°C with anti-mouse secondary antibodies conjugated to AlexaFluor-647 (1:250). In the final half hour of incubation, Hoechst nuclear stain was added (1:5,000). Hemithoraces were mounted in FluoroShield anti-fade fluorescence mounting medium (Abcam, #ab104135) on Superfrost microscope slides (VWR International Radnor, PA) with one spacer coverslip. Fluorescent images of the thorax were acquired using a Nikon AZ100 widefield epifluorescent zoom microscope with a 5X objective and consistent exposure settings between each sample. Images of the myotendinous junction (MTJ) were acquired using a Nikon A1 HD laser scanning confocal microscope with a 40X water objective and consistent settings between each sample. To quantify BPS-integrin density relative to the area of the MTJ, RGB Images were exported from the Nikon Elements software as .TIF files and subsequently analyzed using automatic thresholding methods in ImageJ (NIH) to generate percent area positive for BPS-integrin

staining. All analyses were performed by a single experimenter blinded to the treatment conditions.

2.6 Staging of *Drosophila* pupae:

Pupae were staged by removing white 0 hr APF pupae from the sides of culture vials and allowing them to age to desired pupal stage. To account for developmental accelerations due to temperature shifts or delays with MeHg treatment, stage-specific physical characteristics were also considered, which have been previously described (Bainbridge and Bownes, 1981). Timing of developmental events specific to the IFM were obtained from a transcriptomics resource by Spletter et al., 2018, which was also used to validate our gene-expression patterns (Spletter et al., 2018).

To restrict *kon* induction between 16 – 20 h APF, virgin *Mef2-GAL4*, *Tub-GAL80TS* were crossed to male *UAS-kon* or a genotype control strain (*w1118*) to generate offspring that were maintained at 25°C until 16 h APF and shifted to 29°C from 16 – 20 h APF. The temperature shift relieves the *GAL80TS* repression of the *Mef2-GAL4* transcription factor for 4 h, leading to induction of the *UAS* construct (i.e., *kon*). RNA was collected at the end of induction (20 h APF) to validate *kon* upregulation in gene expression.

2.7 Real time quantitative polymerase chain reaction (RT-qPCR)

Changes of the relative gene expression levels were determined by using the 2^{-Ct} method (Livak and Schmittgen, 2001) using whole-body RNA extracted from staged pupae. All biological replicates are independent samples of 10 pooled pupae. RNA was extracted using the TRIZOL reagent (Invitrogen). The RNA was used to synthesize cDNA using the High-Capacity cDNA Reverse Transcription kit (Fisher #4638813). RT-qPCR was performed in a Bio-Rad CFX96® Real-Time PCR system using iTaq Universal SYBR® Green Supermix (Bio-Rad, # 1725121). Levels of mRNA were normalized to the ribosomal protein *RP49* housekeeping gene. The following primer sequences were used, represented 5'/3':

RP49: AGTATCTGATGCCCAACATCG / TTCCGACCAGGTTACAAGAAC

mys: CAG CAG TCT AAG CTC CTA CTC/GAC TGC GGT TGG ATT TGG AC

kon: GTCAAGTTTCGCACCAGG / CTGATCAGACCGCTCTCC

dGRIP: GCCCATGTTATCCGTTGACC/GTACCCCTTTCTGGTGCCAA

2.8 Total Body Mercury measurement

Total body burden of mercury (T-Hg) was quantified using a DMA-80 Direct Mercury Analyzer (Milestone, Shelton CT). Measured T-Hg was expressed in µg/g (ppm) on a wet weight basis. One biological replicate consisted of pooled groups of 6 – 7 male or female flies. The average and standard deviation for three biological replicates was plotted. For the developmental exposure paradigm, a subset of flies was collected at 0-, 11-, and 30-days PE for measurement, and elimination half time ($t_{1/2}$) was calculated assuming first-order kinetics. For the adult exposure paradigm, a subset of flies was collected at 0-, 4-, and 11-days PE to quantify T-Hg accumulation.

2.9 Statistical analysis

Statistical analyses were done in JMP Pro 14 unless otherwise stated. Comparisons of treatment, age, and/or genotype were evaluated in relation to untreated control strains, the opposite sex, or respective genetically manipulated crosses, or Gal4 > UAS crosses to their relevant control strain or cross, as indicated. Climbing speed after developmental exposure was analyzed using a student's t-test. Climbing speed after adult exposure and landing heights from the flight assay were evaluated using between groups ANOVAs to compare the effects of MeHg treatment, genotype, age, and/or sex, where appropriate. Morphological analyses that quantified relative staining density of BPS-integrin were continuous, parametric variables between two groups, thus compared using a student's t-test. Gene-expression changes were analyzed relative to genotype or untreated controls at the first timepoint (0 h APF), where appropriate, using student's t-tests. When variables did not meet parametric assumptions (i.e., not normally distributed or presented with heteroscedasticity), a non-parametric Mann–Whitney–Wilcoxon or Kruskal-Wallis or test was applied. Values are represented as an average of at least three replicates \pm standard deviation. In all cases, $p < 0.05$ were significant.

RESULTS:

As a first approach to evaluate latent adult-life outcomes of early-life MeHg exposure, we examined longevity. Whereas the mean lifespan in untreated (0 μ M) control flies was 63.99 ± 0.97 days (CI 62.08 – 65.89), flies that had been exposed to low doses of MeHg (2 – 5 μ M) during development lived significantly shorter lives (Figure 2A). The mean lifespan of adult flies reared on food laden with 2 or 5 μ M MeHg was 55.68 ± 0.90 days (CI 53.91 – 57.44) or 48.60 ± 1.07 days (CI 46.51 – 50.684), respectively (Figure 2A). In contrast, with exposure only during the adult stage (0, 50 or 100 μ M MeHg), a significant decrease in lifespan required upwards of 100 times more MeHg in the food (mean lifespan control (0 μ M): 56.88 ± 1.43 days (CI 54.07 – 59.69), 100 μ M: 54.41 ± 0.84 days (CI 52.07 – 56.06)) (Figure 2B). Altogether, these data illustrate the sensitivity of early life exposures to MeHg reflected in deficits in lifespan.

We next sought to determine whether the reduction in lifespan due to developmental exposure to MeHg corresponded with reduced motor function beyond the natural decline expected with age. Following developmental exposure to 0 – 5 μ M MeHg, motor functional tests were evaluated in male and female adult flies. Average climbing speed 4 days post eclosion (PE) was significantly reduced in both males and females (Figure 3A, C). Male flies exposed to 5 μ M MeHg climbed slower than untreated controls (1.33 ± 0.12 cm/s vs. 1.64 ± 0.11 cm/s, $p < 0.05$, Figure 3A, Table S1). MeHg-treated females also climbed slower (1.18 ± 0.09 cm/s vs. 1.36 ± 0.09 cm/s, $p < 0.05$, Figure 3C, Table S1).

Flight ability in 11- and 30-day PE male and female flies was next evaluated. Whereas untreated 11-day d PE flies land in the top 15 cm of the flight column, developmental exposure to 5 μ M MeHg led to a significant drop in landing height measured in distance from the top of the column: in male (10.08 ± 7.55 cm vs. 21.23 ± 14.98 cm, $p < 0.001$) and female flies (14.43 ± 8.18 cm vs. 26.75 ± 16.16 cm, $p < 0.001$) (Figure 3 B, D, Table S3). Female flight was also impaired following developmental exposure to 2.5 μ M MeHg

(14.43 ± 8.18 cm vs 20.75 ± 15.20 cm, $p < 0.01$) (Figure 3D, Table S3). Male and female flies aged to 30 day-PE landed lower in the flight column than their younger 11 day-PE counterparts (males: 10.08 cm vs. 21.20 cm, $p < 0.01$ (Figure 3B, Table S3, S4), females: 14.43 ± 8.18 cm vs. 19.24 ± 12.29 cm, $p < 0.05$, (Figure 3D, Table S3, S4), demonstrating a reduction of landing height with age. However, the combined effects of MeHg treatment and age varied between the sexes. In 30-day PE males, MeHg exacerbated the dose-dependent reduction in landing height from the top of the column observed 11-day PE (Figure 3B). Males treated with 5 µM MeHg and aged to 30-day PE landed further down in the flight column than both untreated controls of the same age group (21.20 ± 11.36 vs. 27.27 ± 16.05 cm, $p < 0.05$), as well as 11-day PE males exposed to 5 µM MeHg (21.23 ± 14.98 vs. 27.27 ± 16.05 cm, $p < 0.05$, (Figure 3B, Table S3, S4). In contrast to the sustained deficits on male flight ability following MeHg exposure, the dose-responsive reduction in flight ability in 11-day PE females was attenuated in their older (30-day PE) counterparts. In 30-day PE females, there was no difference across treatment groups ((Figure 3D, Table S4). Altogether, these results show that MeHg exacerbates the age-dependent decline in flight performance in male flies, and suggest that adult climbing and flight impairments were the result of developmental exposure to MeHg. Nevertheless, it was possible that residual MeHg carried over from the developmental exposure constituted an adult exposure sufficient to affect adult motor function.

To account for the possibility that motor deficits were influenced by an adult exposure secondary to residual MeHg in the body, we monitored total mercury (T-Hg) in the body of adult flies following eclosion. Flies reared on 5 µM MeHg food were recovered on MeHg-free food and whole-body Hg was measured at various timepoints after eclosion (0-, 11-, and 30-day PE). The day of eclosion (0-day PE), 18.27 ± 1.52 ppm and 20.14 ± 0.81 ppm T-Hg was measured in male and female flies, respectively (Figure 4A, D). By day 11 PE, 3.18 ± 0.82 and 3.01 ± 0.72 ppm T-Hg remained in male and female bodies, respectively (Figure 4A, D). By 30-day PE, 0.966 ± 0.26 and 0.868 ± 0.29 ppm T-Hg remained in male and female bodies, respectively (Figure 4A,D). In each sex, more than 80% of the mercury burden had been eliminated from the body by the time of the 11 day-PE flight tests. Almost 50% of the T-Hg was cleared at the time of climbing tests, as calculated from the elimination half-times for males (6.8 days) and females (6.9 days).

It was possible that the T-Hg in adults, albeit much reduced, nevertheless contributed to the observed deficits in climbing (Figure 3A, C) and flight (Figure 3B, D). Therefore, as a secondary measure, flies were exposed to high doses (10 µM or 50 µM) of MeHg exclusively as adults to accumulate T-Hg in the body prior to motor function tests on day 4-PE and day-11 PE (Figure 1B). This was done to recapitulate the T-Hg body burdens leftover from the developmental exposure at the time of climbing and flight testing.

Following adult-exposure to 10 µM for 4 days (*i.e.*, 4-day -PE), male flies accumulated 3.99 ± 0.98 ppm T-Hg, while females accumulated 8.06 ± 0.55 ppm T-Hg (Figure 4B, E). Neither male nor female flies exposed to 10 µM MeHg climbed slower compared to untreated controls (Figure 5A, C). However, exposure to 50 µM MeHg led to much higher T-Hg burdens (Figure 4C, F) and corresponded with reduced climbing speed in males and females compared to untreated controls (Figure 5A, C).

Flight ability and corresponding T-Hg levels (ppm) in 11-day PE flies were also quantified following adult-specific exposure to 0, 10, or 50 μM MeHg. Male and female 11-day PE flies accumulated an average of 9.23 ± 0.78 ppm and 12.31 ± 1.61 ppm T-Hg, respectively, post-exposure to 10 μM (Figure 4B, D). Despite accumulation of T-Hg to levels greater than those observed following the developmental exposure paradigm (Figure 4B, D), there was no significant difference in flight performance in adults exposed to 10 μM compared to untreated controls (Figure 5B, D). However, flight impairments were observed in adults exposed to 50 μM MeHg (Figure 5B, D). These adults were laden with T-Hg levels (ppm) well above those retained in 11-day PE following developmental exposure to 5 μM (Figure 4C, F). Altogether, these results support that the aforementioned deficits in flight, and possibly climbing ability, result from developmental exposure to MeHg; the residual T-Hg following developmental exposure does not constitute a high enough adult exposure (ppm) to appreciably influence adult climbing and flight.

We previously reported that higher levels of developmental MeHg exposure (10 μM) are sufficient to produce a failure in indirect flight muscle (IFM) morphogenesis during pupal metamorphosis (Peppriell et al., 2020). Given the evidence that developmental exposure to 5 μM MeHg contributed to flight deficits, a dose where pupal IFM morphogenesis is not significantly impaired (Peppriell et al., 2020), the sensitivity of developmental events required for adult flight were evaluated at the level of gene expression. Normal flight ability in *Drosophila* relies on proper development of the indirect flight muscles (IFM), including the formation of the myotendinous junction (MTJ) between muscle and the thoracic cuticle to withstand the forceful contractions that produce wingbeats. To determine if 5 μM MeHg affected developmental events of MTJ formation, three core component MTJ genes, *kon-tiki* (*kon*), *Drosophila Glutamate Interacting Protein* (*dGRIP*) and *myospheroid* (*mys*), were analyzed across ten timepoints of pupal development (Figure 6). Gene expression of *kon* was previously shown to be responsive to higher level MeHg (10 μM) exposure (Peppriell et al., 2020). In comparison to untreated controls, *kon* was elevated at 16, 20, and 48 h After Pupa Formation (APF) (Figure 6A). Gene expression of *dGRIP*, the intracellular partner of Kon, was also upregulated at 0, 16, and 48 h APF, trended upwards at 20 h APF, and was suppressed at 90 h APF (Figure 6B). Finally, expression of *mys*, which encodes B-PS integrin, an essential component of MTJ formation, was unaffected across development (Figure 6C).

Given that *mys* gene expression was not changed by MeHg, and that Mys localizes to the MTJ of the IFM, Mys/BPS-integrin antibody staining intensity relative to the MTJ area was used as a proxy to evaluate the integrity of the MTJ in addition to gross morphological assessments of the IFM. Untreated control hemithorax preparations of 11-day PE adults revealed a stereotypical pattern of IFMs, including the six dorsal longitudinal muscles (DLM) spanning the anterior to posterior end of the thorax (Figure 7A, asterisks). The localization of BPS-integrin to both tendon and muscle of each myofibril was reflected in the punctate BPS-integrin+ staining that outlined the curvilinear MTJ of untreated controls (Figure 7C). In comparison to untreated controls, developmental exposure to 5 μM MeHg did not appear to impact gross morphology in hemithorax preparations of 11 day-PE adults (Figure 7B), nor alter the integrity of the MTJ based on relative BPS-integrin distribution (Figure 7D, E).

The above findings indicate that functional deficits in the IFM with early-life MeHg exposure ensue with no apparent gross muscle pathology. We therefore explored the role of underlying molecular constituents in more detail. We chose to further examine *kon*, because our prior study demonstrated that constitutively upregulating *kon* in the developing IFM could hinder adult flight ability without perturbing the IFM (Peppriell et al., 2020). *Kon* is a structural adhesion protein found at the muscle end of the MTJ as well as in muscle costameres and in glia; altering *kon* expression in muscle has the most robust effects in flight compared to altering its expression in other tissues, demonstrated by RNAi-knockdown approaches (Figure S1A). Given the pleotropic requirements of *kon* in muscle, it remained possible that MeHg induced *kon* more globally in muscle to influence adult flight ability.

The restricted upregulation of *kon* at 16–20 hr APF with MeHg (Figure 6A) further suggested a distinct window of susceptibility during muscle development may exist. To assess this possibility, a temperature-inducible transactivation system was used to confine the upregulation of *kon* in muscle (*Mef2Gal4-Gal80ts>UAS-kon*) during the 16 – 20 h after puparium formation (APF) window of IFM development that coincides with timing of MeHg upregulation of *kon* (Figure 6A) by applying a four-hour 29°C heat pulse. Landing height (cm) of adult male (Figure 8A) and female (Figure 8B) *Mef2Gal4-Gal80ts>UAS-kon* flies that did not receive the heat pulse (*Mef2Gal4-Gal80ts>UAS-kon*, 25°C) was not different than genotype control flies (*Mef2Gal4-Gal80ts>w1118*, 25°C or 29°C) (Figure 8A, B, Table S6). Whereas genotype control males typically landed in the top 11 cm of the flight column, a significant drop in average landing height (cm) from the top of the column was observed in *Mef2Gal4-Gal80ts>UAS-kon* flies that received the 29°C heat pulse (10.24 ± 6.64 cm vs. 15.35 ± 15.56 cm, $p < 0.01$) (Figure 8A). However, the observed flight deficits in *Mef2Gal4-Gal80ts>UAS-kon* flies corresponded with an over 30-fold upregulation in *kon* (Figure 8C), which is far in excess of the approximately 2-fold induction elicited by MeHg (Figure 6A). Unexpectedly, in *Mef2Gal4-Gal80ts>UAS-kon* flies that did not receive the heat pulse, there was background *kon* induction (Figure 8C) to levels comparable with those achieved by 5 μ M MeHg treatment (Figure 6A). Muscle-specific *kon* induction at these levels did not correspond with reduced average landing height from the top of the flight column, supporting a model whereby *kon* alone is not sufficient to elicit MeHg flight deficit phenotype seen with 5 μ M MeHg treatments.

Discussion:

Our results reinforce the concept of developmental origins of health and disease (DOHaD) by characterizing an early life sensitivity of *Drosophila* development to MeHg that has latent outcomes in adults. The sensitivity of early life exposure to MeHg is reflected in reduced lifespan as well as motor deficits, and underscores the utility of the *Drosophila* model to resolve underlying developmental targets. We uncovered latent motor behavioral impacts following low-dose exposure to MeHg during development and investigated how effects on the MTJ and muscle may contribute to motor impairments. Our results verified that pupal development is a critical period where the fly is most sensitive to MeHg and established that the latent deficits on adult flight behavior are male-specific. Further assessment will be required to determine whether a component of the IFM (e.g., the MTJ) is sensitive to low-levels of MeHg in a way that contributes to flight defects. This is the first study to

leverage the *Drosophila* model to investigate the latent effects of low-dose methylmercury exposure and combinatorial age \times MeHg effects.

Studies in non-human primates and rodents have identified latent disturbances in sensory as well as motor performance and identified avenues to mitigate latent toxicity via dietary supplementation of selenium or caffeine (Bjorklund et al., 2007) (Heath et al., 2010; Reed et al., 2008; Rice, 1996; Rice and Gilbert, 1995). However, such investigations take years to complete. The comparatively short life-cycle of the fly model lends utility to its continued use to investigate mechanisms of latent toxicity. Here, we demonstrated the first evidence in the fly model where early-life developmental exposure to MeHg reduces lifespan. Continuing to leverage robust attributes of the fly model will likely expedite the discovery of mechanisms of latent MeHg myotoxicity as well as exposure mitigation strategies.

In addition to reduced longevity, we observed age-related loss of flight ability that was exacerbated by MeHg in males only. Consistent with previous reports (Peppriell et al., 2020), we saw that 5 μ M MeHg impaired flight ability in 11 day PE flies (Figure 2B,D). Although 11-day PE females were more sensitive than their male counterparts, female flight impairments do not worsen with continued aging to 30-day PE (Figure 2B). In contrast, landing height in aged (30-day PE) males was reduced further with MeHg treatment and age than age alone, underscoring the male-specificity of the latent impacts of MeHg on flight ability. It has been observed in experimental animal studies as well as epidemiological studies of human infants and children that there are more pronounced MeHg effects in males relative to females (Bjorklund et al., 2007; Cordier et al., 2002; Grandjean et al., 1997; Karagas et al., 2012; McKeown-Eyssen et al., 1983; Rand et al., 2020; Weston et al., 2014). Future studies should investigate the sex and age dependency of MeHg toxicity.

Drosophila IFM, like human skeletal muscle, shows age-related drops in functional performance (i.e. flight) (Miller et al., 2008), which environmental toxicants such as MeHg can potentially exacerbate through a spectrum of molecular, cellular, and structural perturbations. We further examined the hypothesis that MeHg exposure leads to muscle-specific overexpression of *kon*, a critical component of MTJ structure and formation (Peppriell et al., 2020; Perez-Moreno et al., 2014; Weitkunat et al., 2014), to contribute to motor deficits in flight. With this hypothesis, excess *kon* would presumably act to disrupt stoichiometric partnering with its ligand on an opposing tendon cell, destabilizing the MTJ. However, our attempt to increase the dosage of *kon* in muscle at critical developmental time points by genetic means revealed that impaired flight results from a 30-fold induction of *kon* expression (Figure 7C), and that a 2-fold *kon* induction, akin to that seen with MeHg exposure (Figure 5A), has no consequences for adult flight. Thus, our data showing that low-dose MeHg exposure upregulates *kon* suggests that additional factors are operative to contribute to the decrements in adult flight behavior. For example, the *kon* partner *dGRIP* is also upregulated, and a cooperative effect of altering levels of these two factors simultaneously remains to be explored with additional genetic experiments. Unpublished data from our lab show that both RNAi-mediated knockdown of *dGRIP* and *kon* restricted to *Kon*-expressing tissues lead to adult flight deficits.

Our data do not preclude the possibility that *kon* upregulation in other tissues contributes to flight deficits. Indeed, *kon* is also expressed in glia and upregulated to facilitate the glial regenerative response to central nervous system injury in *Drosophila* larvae (Losada-Perez et al., 2016, 2017). Intriguingly, we observed that *kon* is important in glia for flight, where glial-restricted knockdown of *kon* (Repo>UAS-*kon*-RNAi) led to subtle but significant reductions in landing height (Figure S1B). Future studies must explore the responsiveness of glia as it relates to MeHg-related decrements in flight ability and motor function.

Despite its notable strengths, there were several limitations with our study. First, our analysis of latent toxicity on flight behavior was restricted to one wild-type fly strain, *Canton S*. Different wildtype strains of *Drosophila* (e.g., *Hikone R (HR)*) have been shown to exhibit different dose-responsive rates of eclosion, a motor behavior (Rand et al., 2019). Moreover, incorporating additional wildtype genotypes may reveal important gene-environment interactions that influence latent toxicity of MeHg on flight behavior. Indeed, preliminary data from our laboratory indicate that *HR* flies are more sensitive to low-level MeHg in flight tests at 11 days (data not shown). Secondly, we have limited our examination of adult muscle morphology to the DLM fibers of the IFMs. While these fibers are part of the core power generating machinery for flight, as many as 18 pairs of synchronous control muscle are essential for dipteran flight control (Dickinson and Tu, 1997), many of these being difficult to access for phenotyping via microscopy. It is therefore possible that subtle effects on *Kon*, and its partners, could perturb the MTJ in these muscle groups with more selective deleterious effects on flight.

Another limitation was that the present study design did not include longitudinal tracking of adult climbing speed, which is also known to decline with age (Rhodenizer et al., 2008). Our results of climbing speed reduction following developmental MeHg exposure cannot preclude the possible contribution of residual T-Hg, but nonetheless support the inordinate sensitivity of the developing system and shed light on the breadth of latent motor behavior impairments beyond those observed in flight. The fact that developmental MeHg exposure can impact both climbing and flight ability points to common MeHg targets across two distinct neuromuscular systems that power the leg and flight muscles.

Moreover, subcellular mechanisms common to both the leg and flight muscles may mediate latent effects on adult climbing and flight. This could explain the absence of muscle pathology or disfigurement of the IFM MTJ. One possibility is that lower doses of MeHg, which can inhibit myosin-ATPase activity via uncompetitive inhibition (Moreira et al., 2003), disrupt the ATPase-dependent cross-bridge cycle in *Drosophila* IFM. Dysregulated ATPase activity is known to impair the metabolically taxing activity of flight (Kronert et al., 2018). The cross-bridge cycle is an evolutionarily conserved biological process; impacts are likely to be translatable from flies to humans.

In conclusion, we characterize adult-life motor deficits in *Drosophila* flight and climbing behaviors that result from low-dose exposure to MeHg during development and highlight the model's ability to resolve mechanisms, in addition to induction of *kon*, that are operative to contribute to this effect. The latent toxicity of MeHg in *Drosophila* mimics a feature inherent to many studies of MeHg-exposed humans, primates, and rodents, namely, showing male-

biased effects. This connection supports that a shared mechanism contributes to latent MeHg toxicity across phyla and warrants further investigations into strain-, sex- and age-specific adult behavior deficits in *Drosophila*.

Supplementary Material

Refer to Web version on PubMed Central for supplementary material.

Acknowledgements:

We thank the University of Rochester researchers for communal fly husbandry supplies and critical feedback on the project during meetings, especially D. Cory-Slechta, D. Bergstralh, and J. Chakkalakal. We also thank D. Cory-Slechta for feedback on the manuscript. We appreciate the *Drosophila* community as a whole for maintaining curated databases and a culture of sharing, and are grateful to F. Schnorrer for providing us with UAS-kon fly strains.

Funding:

This study was supported by National Institute of Environmental Health Sciences [R01 ES025721 (PI; M.D.R.), P30 ES001247 (co-I; M.D.R.)] and the University of Rochester Environmental Health Center [T32 207026 (A.E.P)].

Citations:

1. Babcock DT, Ganetzky B, 2014. An improved method for accurate and rapid measurement of flight performance in *Drosophila*. *J Vis Exp*(84), e51223. [PubMed: 24561810]
2. Bainbridge SP, Bownes M, 1981. Staging the metamorphosis of *Drosophila melanogaster*. *J Embryol Exp Morphol* 66, 57–80. [PubMed: 6802923]
3. Bakir F, Damluji SF, Amin-Zaki L, Murtadha M, Khalidi A, al-Rawi NY, Tikriti S, Dahahir HI, Clarkson TW, Smith JC, Doherty RA, 1973. Methylmercury poisoning in Iraq. *Science* 181(4096), 230–241. [PubMed: 4719063]
4. Bjorklund O, Kahlstrom J, Salmi P, Ogren SO, Vahter M, Chen JF, Fredholm BB, Dare E, 2007. The effects of methylmercury on motor activity are sex- and age-dependent, and modulated by genetic deletion of adenosine receptors and caffeine administration. *Toxicology* 241(3), 119–133. [PubMed: 17920182]
5. Brand AH, Perrimon N, 1993. Targeted gene expression as a means of altering cell fates and generating dominant phenotypes. *Development* 118(2), 401–415. [PubMed: 8223268]
6. Cordier S, Garel M, Mandereau L, Morcel H, Doineau P, Gosme-Seguret S, Josse D, White R, Amiel-Tison C, 2002. Neurodevelopmental investigations among methylmercury-exposed children in French Guiana. *Environ Res* 89(1), 1–11. [PubMed: 12051779]
7. Day JJ, Reed MN, Newland MC, 2005. Neuromotor deficits and mercury concentrations in rats exposed to methyl mercury and fish oil. *Neurotoxicol Teratol* 27(4), 629–641. [PubMed: 16024222]
8. de Oliveira Ribeiro CA, Nathalie MD, Gonzalez P, Yannick D, Jean-Paul B, Boudou A, Massabuau JC, 2008. Effects of dietary methylmercury on zebrafish skeletal muscle fibres. *Environ Toxicol Pharmacol* 25(3), 304–309. [PubMed: 21783867]
9. Debes F, Budtz-Jorgensen E, Weihe P, White RF, Grandjean P, 2006. Impact of prenatal methylmercury exposure on neurobehavioral function at age 14 years. *Neurotoxicol Teratol* 28(5), 536–547. [PubMed: 17067778]
10. Dickinson MH, Tu MS, 1997. The Function of Dipteran Flight Muscle. *Comparative Biochemistry and Physiology Part A: Physiology* 116(3), 223–238.
11. EPA., U.S., 2019. IRIS Assessment Plan for Methylmercury, U.S. EPA Office of Research and Development. Washington, DC.
12. Gargano JW, Martin I, Bhandari P, Grotewiel MS, 2005. Rapid iterative negative geotaxis (RING): a new method for assessing age-related locomotor decline in *Drosophila*. *Experimental Gerontology* 40(5), 386–395. [PubMed: 15919590]

13. Godfrey KM, Barker DJ, 2001. Fetal programming and adult health. *Public Health Nutr* 4(2b), 611–624. [PubMed: 11683554]
14. Grandjean P, Weihe P, White RF, Debes F, Araki S, Yokoyama K, Murata K, Sorensen N, Dahl R, Jorgensen PJ, 1997. Cognitive deficit in 7-year-old children with prenatal exposure to methylmercury. *Neurotoxicol Teratol* 19(6), 417–428. [PubMed: 9392777]
15. Gunderson JT, Peppriell AE, Vorojeikina D, Rand MD, 2020. Tissue-specific Nrf2 signaling protects against methylmercury toxicity in *Drosophila* neuromuscular development. *Arch Toxicol*.
16. Han SK, Lee D, Lee H, Kim D, Son HG, Yang J-S, Lee S-JV, Kim S, 2016. OASIS 2: online application for survival analysis 2 with features for the analysis of maximal lifespan and healthspan in aging research. *Oncotarget* 7(35).
17. Hanson MA, Gluckman PD, 2014. Early developmental conditioning of later health and disease: physiology or pathophysiology? *Physiol Rev* 94(4), 1027–1076. [PubMed: 25287859]
18. Harada M, 1995. Minamata disease: methylmercury poisoning in Japan caused by environmental pollution. *Crit Rev Toxicol* 25(1), 1–24. [PubMed: 7734058]
19. Heath JC, Banna KM, Reed MN, Pesek EF, Cole N, Li J, Newland MC, 2010. Dietary selenium protects against selected signs of aging and methylmercury exposure. *Neurotoxicology* 31(2), 169–179. [PubMed: 20079371]
20. Hong YS, Kim YM, Lee KE, 2012. Methylmercury exposure and health effects. *J Prev Med Public Health* 45(6), 353–363. [PubMed: 23230465]
21. Iliadi KG, Iliadi NN, Boulianne GL, 2009. Regulation of *Drosophila* life-span: Effect of genetic background, sex, mating and social status. *Experimental Gerontology* 44(8), 546–553. [PubMed: 19481597]
22. Jakobsen JR, Krogsgaard MR, 2021. The Myotendinous Junction—A Vulnerable Companion in Sports. A Narrative Review. *Frontiers in Physiology* 12(259).
23. Karagas MR, Choi AL, Oken E, Horvat M, Schoeny R, Kamai E, Cowell W, Grandjean P, Korrick S, 2012. Evidence on the human health effects of low-level methylmercury exposure. *Environ Health Perspect* 120(6), 799–806. [PubMed: 22275730]
24. Ke T, Prince LM, Bowman AB, Aschner M, 2021. Latent alterations in swimming behavior by developmental methylmercury exposure are modulated by the homolog of tyrosine hydroxylase in *Caenorhabditis elegans*. *Neurotoxicology and Teratology* 85, 106963. [PubMed: 33626374]
25. Kinjo Y, Higaski H, Nakano A, Sakamoto M, Sakai R, 1993. Profile of Subjective Complaints and Activities of Daily Living among Current Patients with Minamata Disease after 3 Decades. *Environmental Research* 63, 241–251. [PubMed: 8243418]
26. Kronert WA, Bell KM, Viswanathan MC, Melkani GC, Trujillo AS, Huang A, Melkani A, Cammarato A, Swank DM, Bernstein SI, 2018. Prolonged cross-bridge binding triggers muscle dysfunction in a *Drosophila* model of myosin-based hypertrophic cardiomyopathy. *Elife* 7.
27. Livak KJ, Schmittgen TD, 2001. Analysis of relative gene expression data using real-time quantitative PCR and the 2⁻(Delta Delta C(T)) Method. *Methods* 25(4), 402–408. [PubMed: 11846609]
28. Losada-Perez M, Harrison N, Hidalgo A, 2016. Molecular mechanism of central nervous system repair by the *Drosophila* NG2 homologue kon-tiki. *J Cell Biol* 214(5), 587–601. [PubMed: 27551055]
29. Losada-Perez M, Harrison N, Hidalgo A, 2017. Glial kon/NG2 gene network for central nervous system repair. *Neural Regen Res* 12(1), 31–34. [PubMed: 28250735]
30. Malm O, Branches FJ, Akagi H, Castro MB, Pfeiffer WC, Harada M, Bastos WR, Kato H, 1995. Mercury and methylmercury in fish and human hair from the Tapajos river basin, Brazil. *Sci Total Environ* 175(2), 141–150. [PubMed: 8560242]
31. Marques RC, Abreu L, Bernardi JVE, Dórea JG, 2016. Neurodevelopment of Amazonian children exposed to ethylmercury (from Thimerosal in vaccines) and methylmercury (from fish). *Environmental Research* 149, 259–265. [PubMed: 26774584]
32. McKeown-Eyssen GE, Ruedy J, Neims A, 1983. Methyl mercury exposure in northern Quebec. II. Neurologic findings in children. *Am J Epidemiol* 118(4), 470–479. [PubMed: 6637974]

33. Miller MS, Lekkas P, Braddock JM, Farman GP, Ballif BA, Irving TC, Maughan DW, Vigoreaux JO, 2008. Aging enhances indirect flight muscle fiber performance yet decreases flight ability in *Drosophila*. *Biophys J* 95(5), 2391–2401. [PubMed: 18515368]
34. Montgomery KS, Mackey J, Thuett K, Ginestra S, Bizon JL, Abbott LC, 2008. Chronic, low-dose prenatal exposure to methylmercury impairs motor and mnemonic function in adult C57/B6 mice. *Behavioural Brain Research* 191(1), 55–61. [PubMed: 18436314]
35. Moreira CM, Oliveira EM, Bonan CD, Sarkis JF, Vassallo DV, 2003. Effects of mercury on myosin ATPase in the ventricular myocardium of the rat. *Comparative Biochemistry and Physiology Part C: Toxicology & Pharmacology* 135(3), 269–275.
36. Myers GJ, Davidson PW, 1998. Prenatal methylmercury exposure and children: neurologic, developmental, and behavioral research. *Environ Health Perspect* 106 Suppl 3, 841–847.
37. Newland MC, Paletz EM, Reed MN, 2008. Methylmercury and nutrition: adult effects of fetal exposure in experimental models. *Neurotoxicology* 29(5), 783–801. [PubMed: 18652843]
38. Newland MC, Rasmussen EB, 2000. Aging unmasks adverse effects of gestational exposure to methylmercury in rats. *Neurotoxicol Teratol* 22(6), 819–828. [PubMed: 11120387]
39. Newland MC, Reed MN, Rasmussen E, 2015. A hypothesis about how early developmental methylmercury exposure disrupts behavior in adulthood. *Behav Processes* 114, 41–51. [PubMed: 25795099]
40. Newland MC, Reile PA, Langston JL, 2004. Gestational exposure to methylmercury retards choice in transition in aging rats. *Neurotoxicol Teratol* 26(2), 179–194. [PubMed: 15019952]
41. Peppriell AE, Gunderson JT, Vorojeikina D, Rand MD, 2020. Methylmercury myotoxicity targets formation of the myotendinous junction. *Toxicology* 443, 152561. [PubMed: 32800841]
42. Perez-Moreno JJ, Bischoff M, Martin-Bermudo MD, Estrada B, 2014. The conserved transmembrane proteoglycan Perdido/Kon-tiki is essential for myofibrillogenesis and sarcomeric structure in *Drosophila*. *J Cell Sci* 127(Pt 14), 3162–3173. [PubMed: 24794494]
43. Prince LM, Rand MD, 2017. Notch Target Gene *E(spl)mdelta* Is a Mediator of Methylmercury-Induced Myotoxicity in *Drosophila*. *Front Genet* 8, 233. [PubMed: 29379520]
44. Rand MD, Conrad K, Marvin E, Harvey K, Henderson D, Tawil R, Sobolewski M, Cory-Slechta DA, 2020. Developmental exposure to methylmercury and resultant muscle mercury accumulation and adult motor deficits in mice. *Neurotoxicology* 81, 1–10. [PubMed: 32735808]
45. Rand MD, Vorojeikina D, Peppriell A, Gunderson J, Prince LM, 2019. *Drosophotoxicology: Elucidating Kinetic and Dynamic Pathways of Methylmercury Toxicity in a Drosophila Model*. *Frontiers in Genetics* 10(666).
46. Reed MN, Banna KM, Donlin WD, Newland MC, 2008. Effects of gestational exposure to methylmercury and dietary selenium on reinforcement efficacy in adulthood. *Neurotoxicol Teratol* 30(1), 29–37. [PubMed: 18096364]
47. Reuhl KR, 1991. Delayed expression of neurotoxicity: the problem of silent damage. *Neurotoxicology* 12(3), 341–346. [PubMed: 1745427]
48. Rhodenizer D, Martin I, Bhandari P, Pletcher SD, Grotewiel M, 2008. Genetic and environmental factors impact age-related impairment of negative geotaxis in *Drosophila* by altering age-dependent climbing speed. *Experimental gerontology* 43(8), 739–748. [PubMed: 18515028]
49. Rice DC, 1996. Sensory and cognitive effects of developmental methylmercury exposure in monkeys, and a comparison to effects in rodents. *Neurotoxicology* 17(1), 139–154. [PubMed: 8784825]
50. Rice DC, Gilbert SG, 1995. Effects of developmental methylmercury exposure or lifetime lead exposure on vibration sensitivity function in monkeys. *Toxicol Appl Pharmacol* 134(1), 161–169. [PubMed: 7676451]
51. Sheehan MC, Burke TA, Navas-Acien A, Breyse PN, McGready J, Fox MA, 2014. Global methylmercury exposure from seafood consumption and risk of developmental neurotoxicity: a systematic review. *Bull World Health Organ* 92(4), 254–269F. [PubMed: 24700993]
52. Sorensen N, Murata K, Budtz-Jorgensen E, Weihe P, Grandjean P, 1999. Prenatal methylmercury exposure as a cardiovascular risk factor at seven years of age. *Epidemiology* 10(4), 370–375. [PubMed: 10401870]

53. Spletter ML, Barz C, Yeroslaviz A, Zhang X, Lemke SB, Bonnard A, Brunner E, Cardone G, Basler K, Habermann BH, Schnorrer F, 2018. A transcriptomics resource reveals a transcriptional transition during ordered sarcomere morphogenesis in flight muscle. *Elife* 7.
54. Spyker JM, Sparber SB, Goldberg AM, 1972. Subtle consequences of methylmercury exposure: behavioral deviations in offspring of treated mothers. *Science* 177(4049), 621–623. [PubMed: 5049306]
55. Trotter JA, Hsi K, Samora A, Wofsy C, 1985. A morphometric analysis of the muscle-tendon junction. *The Anatomical Record* 213(1), 26–32. [PubMed: 4073558]
56. UN, 2019. Global Mercury Assessment: 2018, UN environmental Programme, Chemicals and Health Branch, Switzerland.
57. Usuki F, Yasutake A, Matsumoto M, Umehara F, Higuchi I, 1998. The effect of methylmercury on skeletal muscle in the rat: a histopathological study. *Toxicol Lett* 94(3), 227–232. [PubMed: 9609326]
58. Weiss B, Clarkson TW, Simon W, 2002. Silent latency periods in methylmercury poisoning and in neurodegenerative disease. *Environ Health Perspect* 110 Suppl 5, 851–854. [PubMed: 12426145]
59. Weitkunat M, Kaya-Copur A, Grill SW, Schnorrer F, 2014. Tension and force-resistant attachment are essential for myofibrillogenesis in *Drosophila* flight muscle. *Curr Biol* 24(7), 705–716. [PubMed: 24631244]
60. Weitkunat M, Schnorrer F, 2014. A guide to study *Drosophila* muscle biology. *Methods* 68(1), 2–14. [PubMed: 24625467]
61. Weston HI, Sobolewski ME, Allen JL, Weston D, Conrad K, Pelkowski S, Watson GE, Zareba G, Cory-Slechta DA, 2014. Sex-dependent and non-monotonic enhancement and unmasking of methylmercury neurotoxicity by prenatal stress. *Neurotoxicology* 41, 123–140. [PubMed: 24502960]
62. Yorifuji T, Takaoka S, Grandjean P, 2018. Accelerated functional losses in ageing congenital Minamata disease patients. *Neurotoxicol Teratol* 69, 49–53. [PubMed: 30102975]

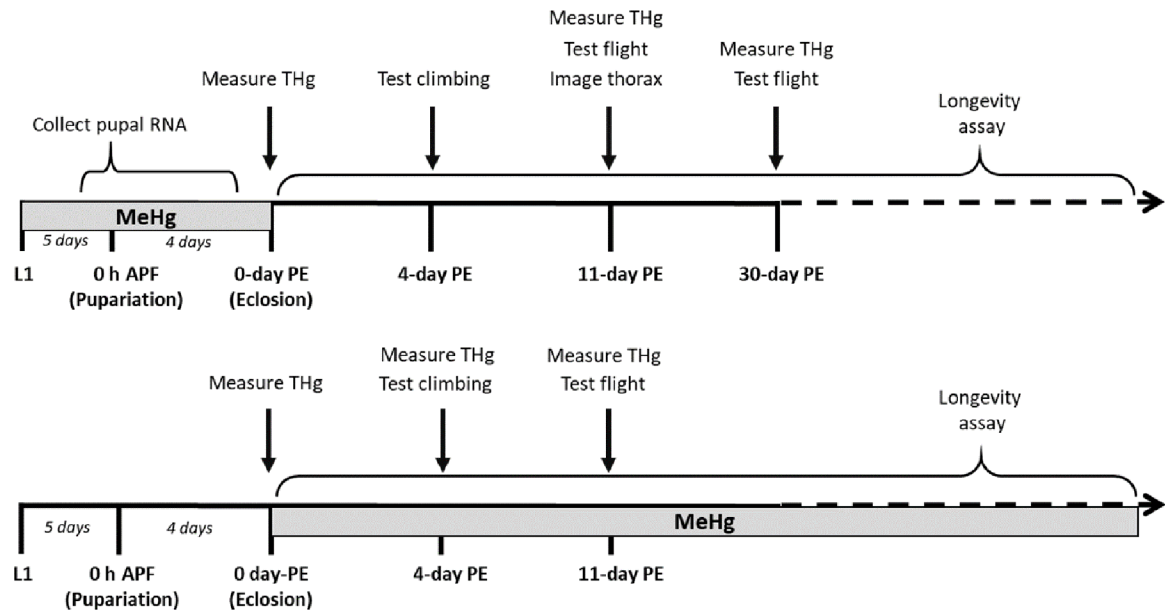


Figure 1a: Experimental Timelines.

A) The developmental MeHg exposure paradigm spans first-instar larva (L1) through 0 h After Pupa Formation (h APF) through eclosion, after which flies are separated by sex and transferred to MeHg-free recovery food leading up to climbing assays 4-days PE, as well as flight assays 11- and 30- days PE. Muscle structure was examined at 11-day PE via immuno-fluorescence microscopy. RNA was harvested from staged pupae for RT-qPCR. Average T-Hg levels (ppm) were measured in male and female adults 0– 11-, and 30-days PE. **B)** The adult exposure paradigm spans eclosion through the time of climbing assays 4-days PE and flight 11-days PE. Average T-Hg levels (ppm) were measured in male and female adults 0-, 4-, and 11-days PE.

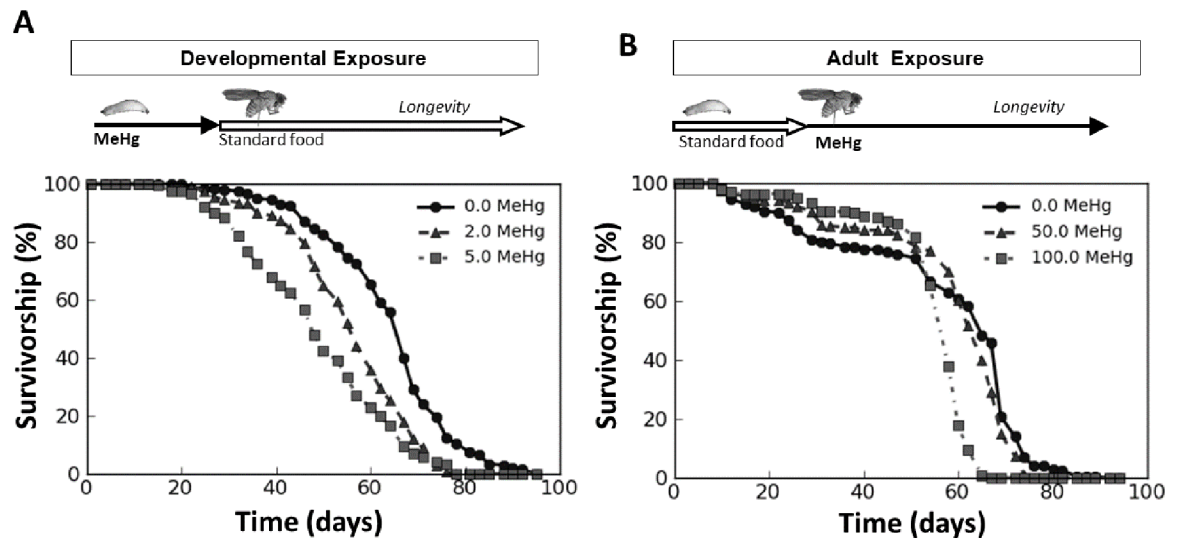


Figure 2: Longevity of adult male flies following developmental and adult-specific exposure to MeHg.

Each point represents the percent of 200 initial flies alive across time (days) following **A**) developmental (larval) exposure to 0 (circles), 2 (triangles), or 5 μM MeHg (squares) and **B**) exposure to 0 (circles), 50 (triangles), or 100 μM MeHg (squares) throughout adulthood, lasting from eclosion until death. The developmental exposure extended from larva through pupal life, ending at eclosion (solid arrow in A), whereupon flies were changed to standard MeHg-free food (open arrow in A). Adult exposure (solid arrow in B) occurred after rearing on MeHg-free food (open arrow in B).

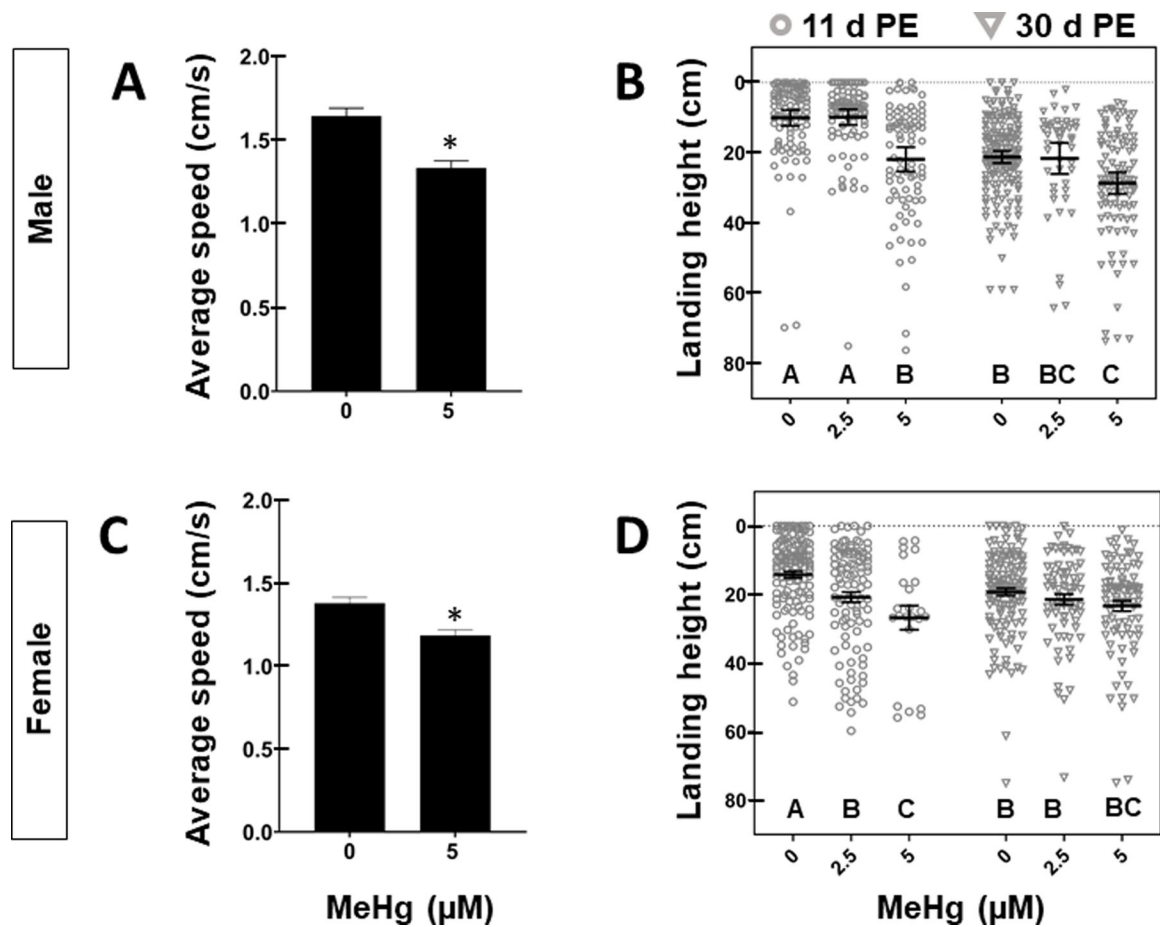


Figure 3: Motor behavioral effects in adult flies following developmental exposure to MeHg. Average \pm SD climbing speed (cm/s) for **A**) Male and **C**) Female adults 4-days PE exposed to 0 or 5 μM MeHg. Asterisks (*) indicate statistical significance (student's t-test, $p < 0.05$, $n = 30$ flies/group). Landing height of **(B)** male and **(D)** female 11- or 30-day PE adults after larval exposure to 0, 2.5, or 5 μM MeHg. Horizontal bars represent mean landing height \pm SEM for each group ($n = 47 - 168$ flies per treatment, letters indicate pair-wise significant differences where $p < 0.05$, Two-Way ANOVA, Tukey's HSD post-hoc).

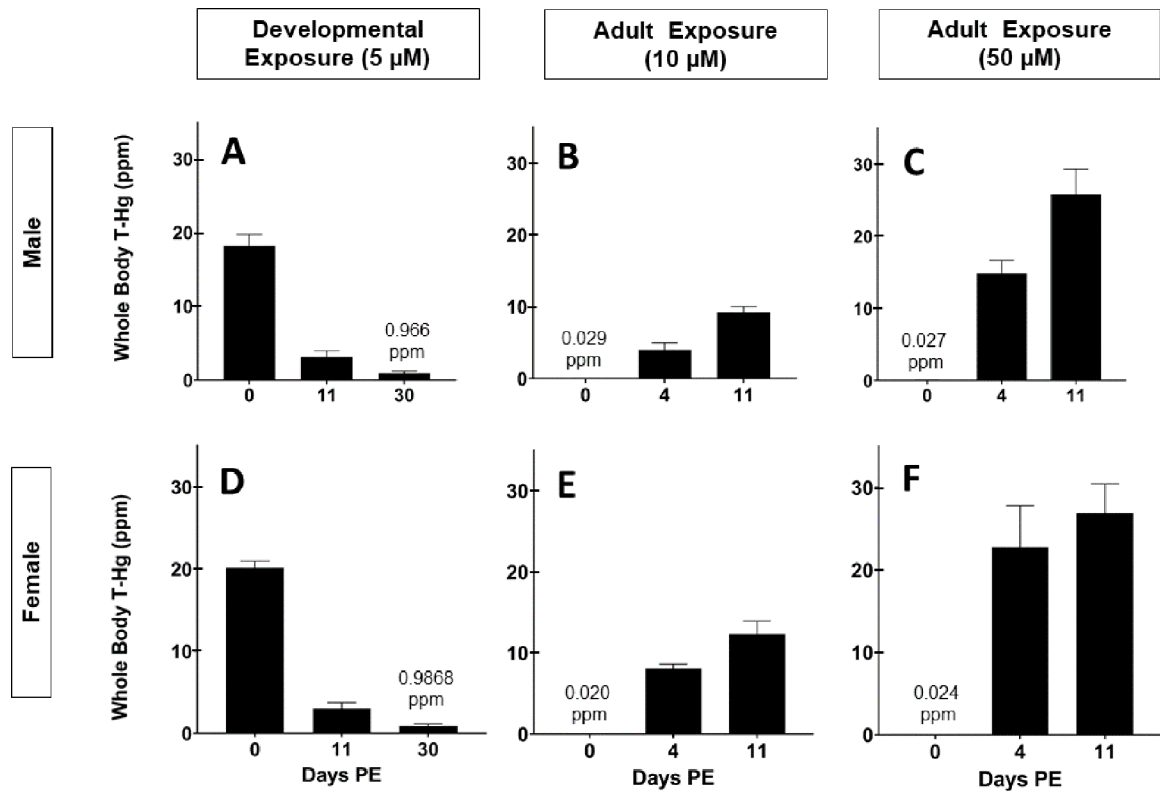


Figure 4: Total mercury (T-Hg) body burdens in male and female adult flies with different exposure paradigms.

Average \pm SD body burden in adult (A) male and (D) female flies 0-, 11-, and 30-day PE following developmental exposure to 5 μ M MeHg. Average \pm SD body burden in adult (B, C) male and (E, F) female flies 0-, 4-, and 11-day PE following adult exposure to (B, E) 10 or (C, F) 50 μ M MeHg.

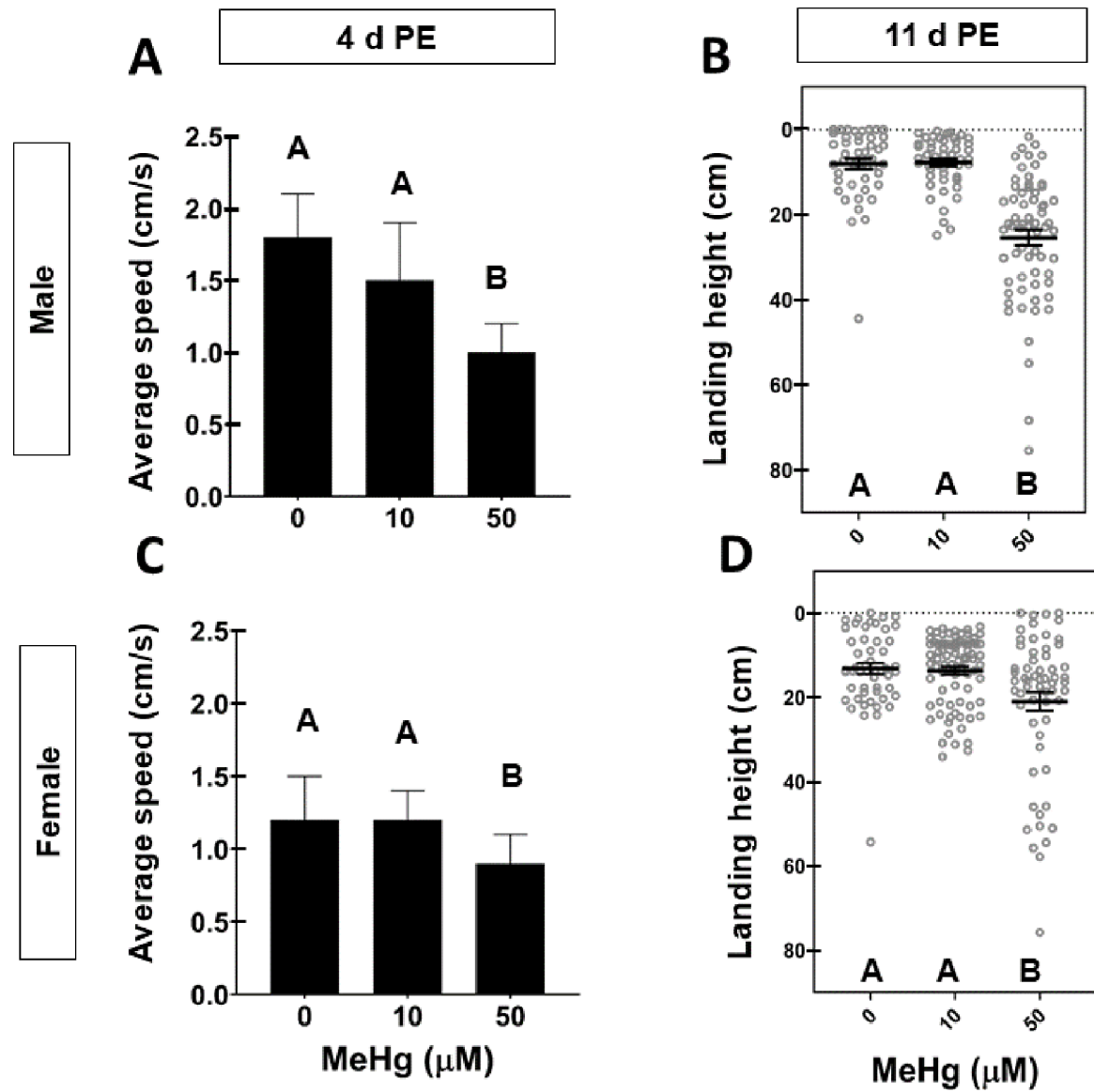


Figure 5: Motor behavioral effects in adult flies following adult exposure to MeHg. Average \pm SD climbing speed (cm/s) for **A**) Male and **C**) Female adults 4-days PE exposed to 0, 10, or 50 μM MeHg. Letters indicate pair-wise significant differences where $p < 0.05$, One-Way ANOVA, $n = 30$ flies/group. Landing height of **(B)** male and **(D)** female 11-day PE adults after adult exposure to 0, 10, or 50 μM MeHg. Horizontal bars represent mean landing height \pm SEM for each group and letters indicate pair-wise significant differences where $p < 0.05$, One-Way ANOVA, $n = 52 - 86$ flies per group.

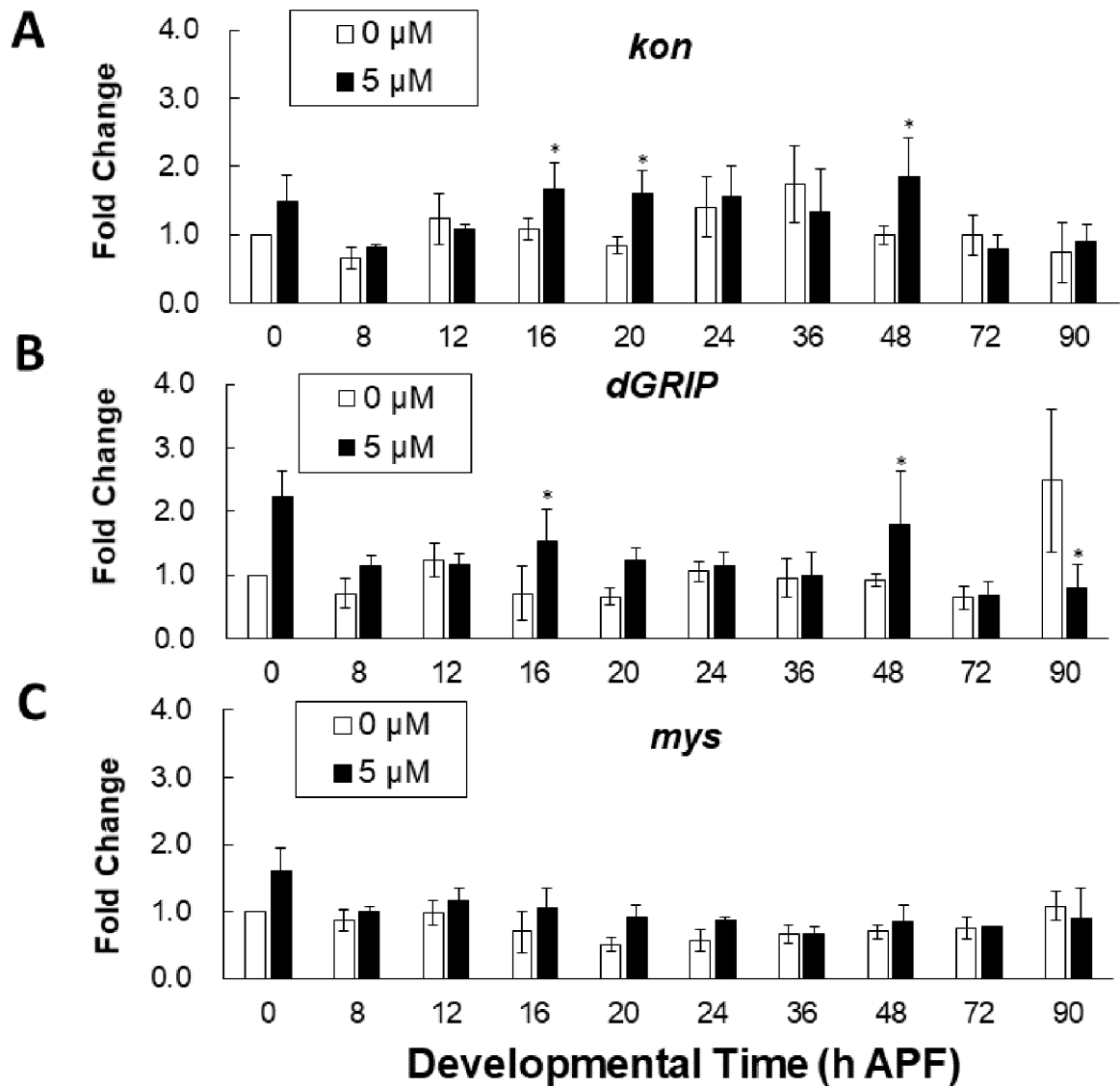


Figure 6: Effect of 5 μM MeHg on gene expression of MTJ genes.

Gene transcript levels with and without 5 μM MeHg of (A) *kon* (B) *dGRIP* (C) and *mys* (BS-integrin) analyzed by RT-qPCR at the indicated pupal developmental timepoints. Each data point is normalized to untreated at the first timepoint (0 h APF). (n = 3; student's t-test, *p < 0.05 in comparison to 0 μM exposure).

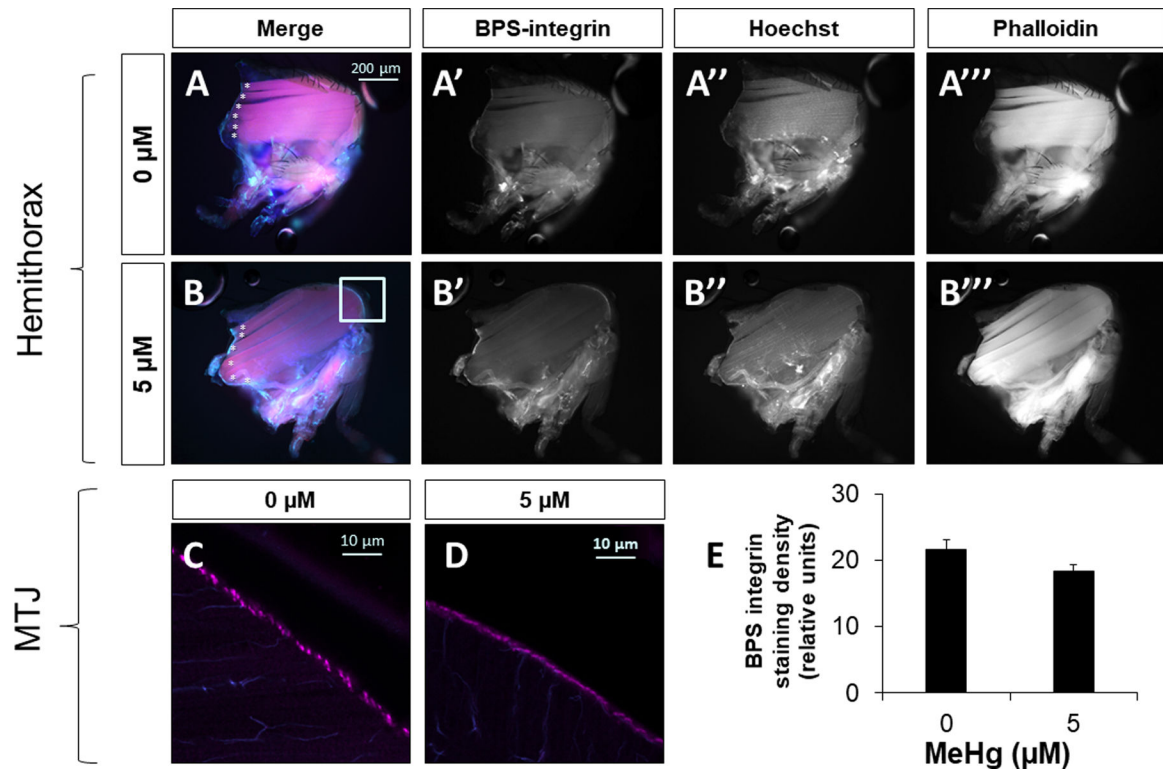


Figure 7: Muscle morphology and MTJ structure in adult flies following developmental exposure to 5 μM MeHg.

Representative images of hemithorax preparations of **A)** untreated control (0 μM) or **B)** 5 μM MeHg-treated adult female flies 11 day-PE visualized with BPS-integrin staining, Hoescht (nucleii), and phalloidin (muscle fibers). Representative images of the MTJ of **C)** untreated control (0 μM) or **D)** 5 μM MeHg-treated adult female 11-day PE flies stained with BPS-integrin and visualized at 40X via confocal microscopy **E)** the quantification of BPS staining density relative to the MTJ area ($n = 10$ hemithoraces/treatment).

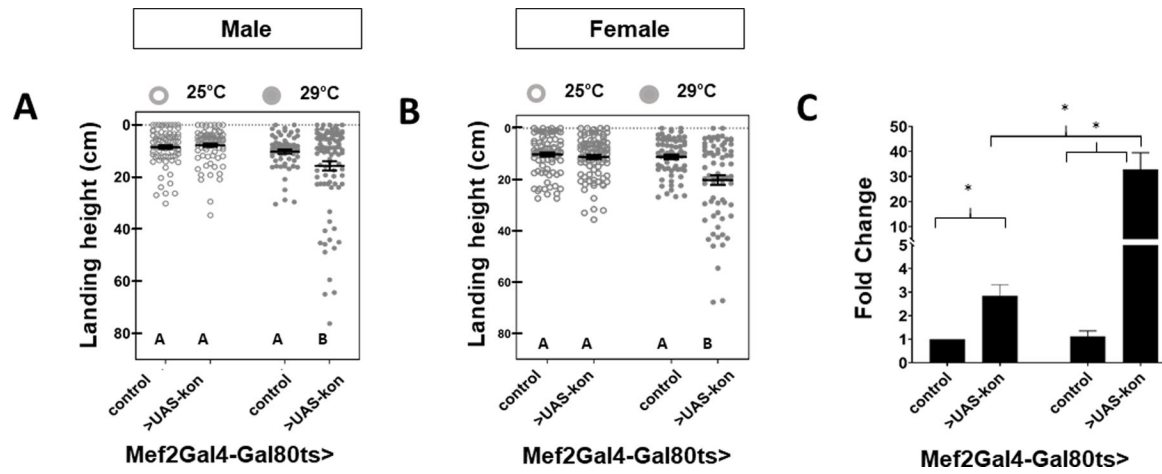


Figure 8: Flight ability in adult flies following temporally restricted upregulation of *kon*.

A temperature-sensitive transactivation system was used to selectively induce *kon* gene expression during the 16 – 20 h APF window of pupal development. Landing height (cm) from the top of the column was quantified in **A**) male and **B**) female flies (Mef2Gal4-Gal80ts >w1118 (control) or >UAS-*kon*) that were reared at 25°C for the entire duration of development or shifted to 29°C for four hours during development. **C**) Average fold change \pm SD in *kon* gene expression in 20 h APF pupae was assessed by RT-qPCR at the end of the induction period (i.e., 20h APF).